Proceedings of the Fifteenth International Conference on
Computational Structures Technology
Edited by: P. Iványi, J. Kruis and B.H.V. Topping
Civil-Comp Conferences, Volume 9, Paper 4.6
Civil-Comp Press, Edinburgh, United Kingdom, 2024
ISSN: 2753-3239, doi: 10.4203/ccc.9.4.6

Topology and Sizing Optimisation of Cowcatcher for Enhancing Post-Derailment Passive Safety Performance

Z. Tang, Z. Peng, S. Liu, T. Chen and Z. Qu

State Key Laboratory of Rail Transit Vehicle System, Southwest Jiaotong University
Chengdu, China

Abstract

The train cowcatcher not only sweeps aside animals, debris, or objects obstructing the tracks, preventing damage to a train and reducing the risk of derailment, but it also serves as a passive safety protection mechanism after a derailment. However, due to intense impact forces, the cowcatcher may sustain severe structural damage, potentially compromising its passive safety protection capability. To address this issue, this paper employs a collaborative optimisation approach to conduct topology and sizing optimisation of the cowcatcher, aiming to reduce its mass while enhancing structural strength and passive safety protection performance after a derailment. Validation tests were conducted for both pre- and post-optimized cowcatchers in the derailment simulations. The results indicate that the post-optimized cowcatcher exhibits stronger structural stability, and its passive safety protection capability is improved.

Keywords: passive train safety; post-derailment; vehicle cowcatcher; structural optimisation; topology optimisation; sizing optimisation.

1 Introduction

The primary function of a train cowcatcher is to sweep aside animals, debris, or objects obstructing the tracks [1], preventing damage to the train and reducing the risk of derailment [2]. Therefore, its passive safety capability is often overlooked in train derailment simulation analysis and field test research. However, photographs taken at accident scenes, as shown in Figure 1, illustrate that the cowcatcher also plays a role

in passive safety protection after a derailment, by restricting the train's movement laterally and longitudinally.

Inspired by this, from the perspective of cowcatcher's passive safety protection capability, given that the cowcatcher may sustain damage under high speed derailment [3] and lose its passive safety capability due to significant impacts, this study focuses on the topology and sizing optimisation of the cowcatcher based on its collision response, utilizing the topology and sizing optimisation for the structure design. Initially, topology optimisation determines the best material distribution within a given design domain. Then, secondary engineering interpretations derive the optimal material distribution configuration. Sizing optimisation follows to achieve the best structure solution. Finally, structural verification analysis confirms the effectiveness of the optimized structure.

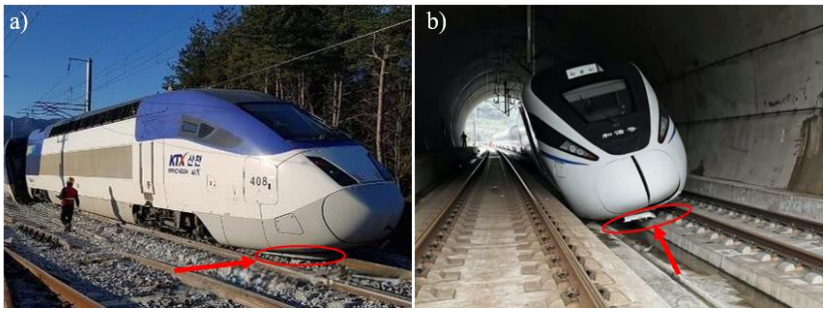

Figure 1 Derailment accidents: the contact between the cowcatcher and the rail

The concept of structural optimisation is to establish a mathematical model for the structure, which includes selecting design variables, defining objective functions, and setting constraints[4]. Under these constraints, the goal is to find the optimal structural design that satisfies the objective. Structural optimisation design methods include the main three types: topology optimisation, sizing optimisation and shape optimisation [5, 6, 7]. The structural optimisation design method has been developed over time in many areas, such as civil engineering about high-rise building [8] and renewable energy industry [9], and is also gradually being widely applied in rail transportation. Chen et al. [10] optimized the windowed structure of the main specific energy absorption (SEA) components, resulting in a 6% increase in SEA and a 7% reduction in peak force. Kuczek et al. [11] employed the SIMP method to lightweight the side walls of railway vehicles according to EN 12663 standards, achieving a notable improvement in light-weighting. Mrzygd et al. [12] introduced a uniform optimisation method for enhancing the structural durability of high-speed train. Their efforts in structural optimisation led to improved passive safety performance of the locomotive body structure.

2 FE modelling and optimisation methods

2.1 FE modelling

This section introduces the FE models, with an emphasis on the cowcatcher. As shown in Figure 2, the cowcatcher is fixedly connected to the chassis through bolts, and

consists of cowcatcher deflectors, connection ribs, buffer plate supports, cowcatcher stopper and other structures.

The cowcatcher deflector is the outermost structure that is in direct collision contact with obstacles [13, 14]. The connection rib serves as the structure connecting the cowcatcher deflector and the buffer plate, and is also the main force transmission structure. The buffer plate is composed of five aluminium alloy thin-walled plates arranged in the front and the back. In the event of a direct frontal collision, the structure can collapse and absorb energy. Cowcatcher stoppers are used to remove obstacles on the track and are located directly above the rail surfaces on both sides. The main material properties of the cowcatcher are shown in Table 1.

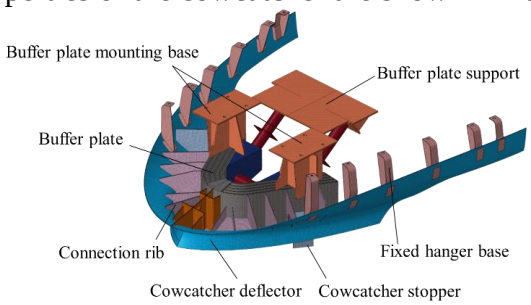

Figure 2 Cowcatcher FE model

Table 1 The main material properties of the cowcatcher

Material	Density /kg.m^{-3}	Young's Modulus / GPa	Poisson ratio	Yield strength /MPa	Shear Modulus /GPa
Q460E	7.83×10^{3}	210	0.3	460	10
6005A_T6	2.70×10^{3}	70	0.3	225	1.13

Additionally, FE models of the track, car body, and bogie, are established to simulate the post-derailment behaviour and to test the performance of the cowcatcher, as shown in Figure 3.

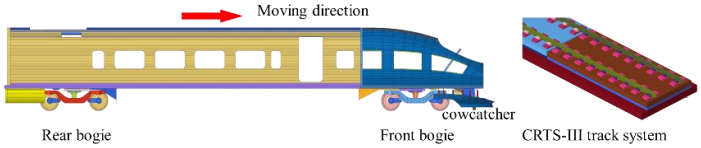

Figure 3 The FE models of carbody, bogie, and non-ballasted track

2.2 Optimisation method and theories

The optimisation methods discussed in this article entails initially conducting topological analysis and optimisation of the geometric shape of the cowcatcher. Subsequently, sizing optimisation is performed to achieve collaborative optimisation design, thereby achieving the objective of enhancing the derailment suppression performance of the cowcatcher.

2.2.1 Topology optimisation method

Topology optimisation involves generating an optimized distribution of material elements within a specified design domain to achieve the best structural performance while adhering to the given responses and constraints [15]. Currently, there are three main topology optimisation methods: the Hybrid Cellular Automata method (HCA) [16], Equivalent Static Loads (ESL) [17], and the Variable Density Method (Solid Isotropic Material with Penalization, SIMP) [18].

The SIMP is a prevalent technique appreciated for its stable iterative process and high optimisation efficiency [19]. The core concept of the SIMP method is to assume that the density of structural elements varies continuously between 0 and 1 [20]. By establishing a relationship between element density and material properties, changes in element density affect the performance of the structure. This approach enables the acquisition of structures with optimal physical properties. The general math model of SIMP is as follows:

$$\begin{aligned} &\text{find: } x_i(i = 1,2,\dots,N), \forall i \in \Omega \\ &\text{min: } C(x) = C(\boldsymbol{u}(x), x) = \int_{\Omega} c(\boldsymbol{u}(x), x) dV \\ &\text{s.t. } \begin{cases} G_0(x) = \int_{\Omega} x_i dV - V_0 \leqslant 0 \\ G_r(\boldsymbol{u}(x), x) \leqslant 0, r = 1,2,\dots M \\ 0 < x_{min} < x_i \leqslant 1 \end{cases} \end{aligned} \tag{1}$$

where Ω is the design domain，N is the number of the elements，x_i is the relative density of the i^{th} element, C is the objective function, $\boldsymbol{u}$ is the state domain, V is the structural volume, G_0 is the structural volumetric constraint, V_0 is the max volume after optimisation, G_r is the r^{th} additional constraint, M is the number of additional constraints，x_{min} is the min relative density of the material.

In this paper, when conducting topology optimisation of the cowcatcher, the objective function is set to maximize stiffness, while maintaining a volume constraint of 35%. Therefore, Eq (1) can be transformed into the following Eq (2):

$$\begin{aligned} &\text{find: } x_i(i = 1,2,\dots,N), \forall i \in \Omega \\ &\text{min: } C(x) = \boldsymbol{F}^T \boldsymbol{U} \\ &\text{s.t. } \begin{cases} G_0(x) = \sum_{i=1}^{N} x_i - V_0 \leqslant 0 \\ \boldsymbol{F} = \boldsymbol{K}\boldsymbol{U} \\ 0 < x_{min} < x_i \leqslant 1 \end{cases} \end{aligned} \tag{2}$$

where $\boldsymbol{F}$ is the load vector, $\boldsymbol{U}$ is the displacement vector, $\boldsymbol{K}$ is the stiffness matrix, and the optimized V_0 is $0.35V$.

2.2.2 Sizing optimisation method

Sizing optimisation, also referred to as parameter optimisation, typically utilizes the properties of structural components as design variables [21]. These variables may

include the thickness of shell elements, the moment of inertia and the area of beam sections, the stiffness of spring elements, the magnitude of loads, etc. This method is commonly employed for further refinement during the detailed design phase.

In this study, during sizing optimisation of the cowcatcher, minimizing its mass is established as the objective function. Considering various operating conditions, the mathematical model for sizing optimisation can be expressed as follows:

$$\begin{cases} \text{find } X = \{x_1, x_2, \cdots, x_n\}^{\mathrm{T}} \\ minM(X) \\ \sigma_{max,\,\mathrm{case}} \leqslant \sigma_{\mathrm{case}}^{U}, \mathrm{case} = 1,2,3,4 \\ D_i^L \leqslant D_i \leqslant D_i^U, i = 1,2,\cdots,n \end{cases} \tag{3}$$

where M is the mass of the cowcatcher design domain, case refers to different load cases, $\sigma_{max,\,\mathrm{case}}$ is the maximum stress under different loads, D_i is the thickness of the selected plate between lower L and upper U limit, and X is the selected design domain.

3 Topology optimisation of the cowcatcher

3.1 Topology optimisation model and optimisation condition design

3.1.1 Topology optimisation model

Based on the stress and strain results of the cowcatcher during the post-derailment, as shown in Figure 4, it is evident that significant stress concentrations and plastic deformations occur in both the buffer plate and the connection rib during the collision between the cowcatcher and the rail.

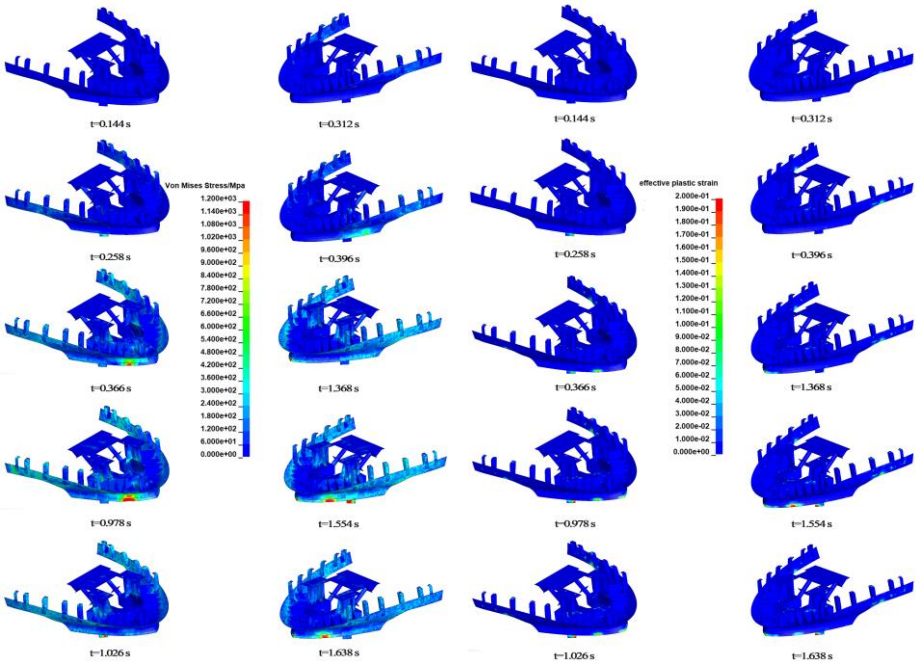

Figure 4 The stress and strain contours of the cowcatcher during post-derailment collisions

Since the connection rib is the primary structure for stress transmission, conducting topology optimisation on it will be advantageous for optimizing force transmission., thereby minimizing the stress transferred to the interior side of the cowcatcher. The cowcatcher deflector is a structure that directly bears impact forces and is also included in the optimisation design domain.

Based on the stress-strain analysis during post-derailment collisions, the optimized domain for the topology optimisation model has been determined. As illustrated in Figure 5, the purple region is the design domain and the grey one is non-design domain. The size and quality of mesh elements in the topology optimisation model will influence the optimisation results. By partitioning various mesh elements of different sizes for preliminary optimisation, it was ultimately decided to discretize the cowcatcher model using 8 mm size mesh elements.

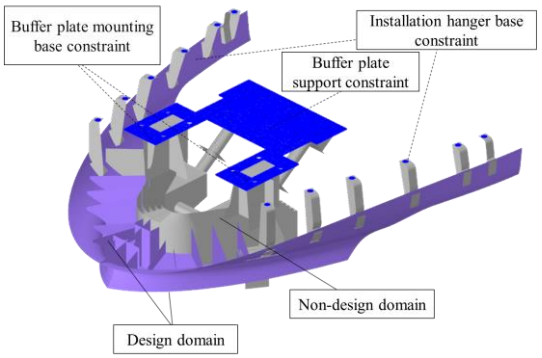

Figure 5 The topology optimisation model of the cowcatcher

3.1.2 Optimisation condition design

Based on the collision outcomes of train derailments at different speeds, the contact conditions of the cowcatcher during derailment at 50 km/h were selected as the basis for topology optimisation. The maximum contact force in this scenario was increased by 10%, and this value was used as the applied load under the optimized condition.

The longitudinal contact force and vertical contact force experienced by the cowcatcher in the post-derailment are set as the 1st and 2nd optimisation conditions, respectively. The compression loads on the frontal and side end-faces specified in the standard "TB/T 3500-2018" are designated as the 3rd and 4th optimisation conditions. The multiple loading conditions applied to the cowcatcher's topology optimisation model are illustrated in Figure 6.

In the topology optimisation of the cowcatcher, the mesh element density in the optimized domain acts as the design variable, the objective function is set to minimize the compliance, and the constraint is that the volume function in the given design domain does not exceed 35%. In addition, since there are multiple optimisation working conditions, topology optimisation under multi-working conditions is carried out based on weighted compliance response. In the weighted compliance response, the ratio of the weighting coefficient between each working condition and the compliance response has a direct impact on the optimisation results. In order to avoid

a certain working condition dominating the optimisation results, usually the weighting coefficients of all working conditions are set to 1 for a round of initial optimisation, and then the appropriate weighting coefficients for each optimisation working condition are determined based on the obtained response results.

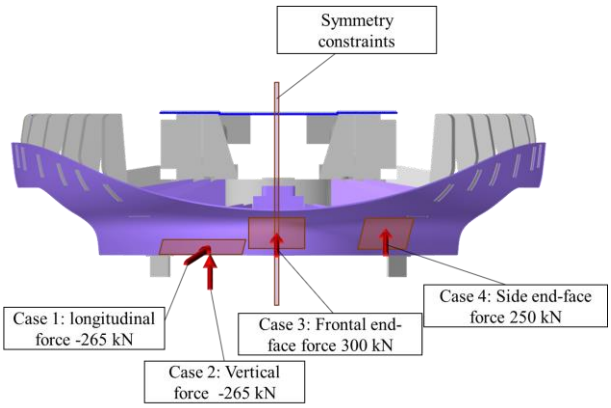

Figure 6 Schematic diagram of load conditions cases

To effectively address material accumulation issues in the optimisation results, it is recommended to set the minimum member size at three times the average size of the model mesh and the maximum mesh size at six times the average size of the model mesh. Additionally, to ensure symmetry in the optimisation results, a plane symmetry constraint was applied within the optimized area, with the central symmetry line of the cowcatcher serving as the coordinate system.

It can be observed from Table 2 that the compliance response for each subcase in the initial optimisation can be calculated. The weighted coefficient ratio of the 4 weighted compliance responses is 0.857: 0.038: 1.000: 0.847. To achieve more precise results, the convergence tolerance of the objective function is set to 5×10^{-4}, and the maximum number of iterations is set to 75.

Table 2 Initial optimisation response results

Subcase	Initial Weight	Compliance	Residual Strain Energy Ratio	Initial Weight*Compliance
1	1.0	1.494037×10^{5}	4.205342×10^{12}	1.494037×10^{5}
2	1.0	3.404240×10^{6}	-2.385594×10^{12}	3.404240×10^{6}
3	1.0	1.280837×10^{5}	-8.430735×10^{12}	1.280837×10^{5}
4	1.0	1.511550×10^{5}	$2.156480E\times10^{12}$	1.511550×10^{5}

3.2 Analysis of topology optimisation results

Figure 7 shows the curve of the objective function value changing with the number of iteration steps. It can be seen that the objective function reaches the specified tolerance and converges after 59 iterations. In order to obtain more discrete results, the optimisation engine will automatically adjust the value of the penalty factor during the optimisation process.

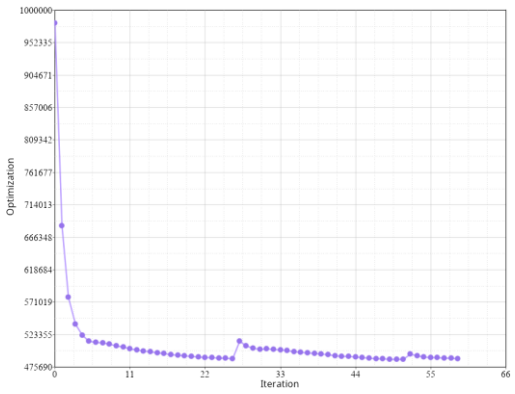

Figure 7 Topology optimisation objective function convergence curve

Figure 8 shows the element density contour. The red ones represent the high-density elements that need to be retained and the blue ones are low-density elements that will be removed. As the number of iteration steps increases, the corresponding elements in the design domain of the cowcatcher are gradually deleted. Among them, the cowcatcher deflector structure retains a larger number of elements between both sides of the cowcatcher rubber, and the connection rib retains the force transmission. The iterative process finally obtained better optimisation results, which provided an effective reference for further improvement of the cowcatcher structure.

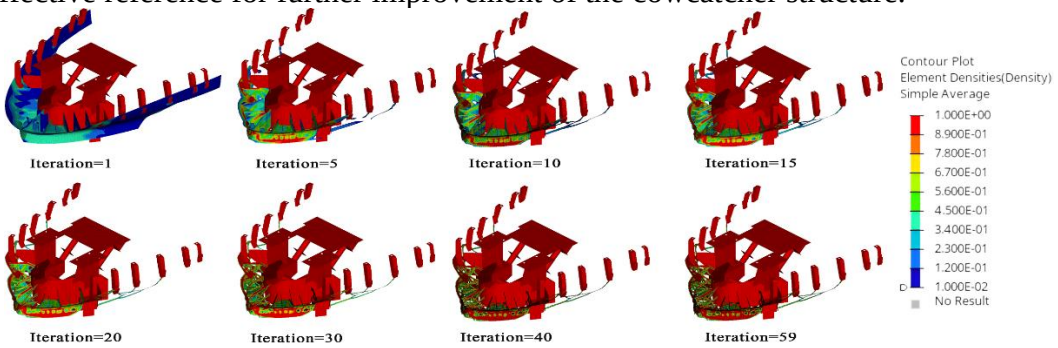

Figure 8 Topology optimisation at specific iteration steps

The optimized structure result of the cowcatcher is shown in Figure 9. Topology optimisation is just for the conceptual design stage in structural optimisation, and its results can only serve as reference for the final design structure. Secondary engineering design of the obtained results is required to improve the structure better.

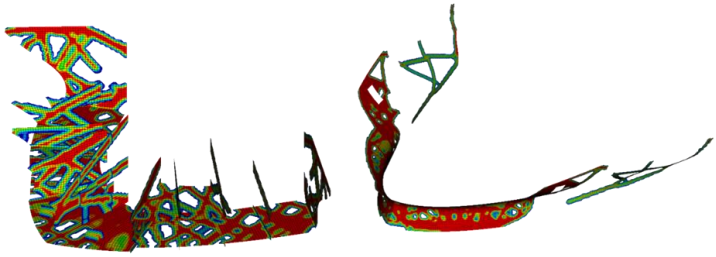

(a) The topology result of the connected plate (b) The topology result of the cowcatcher deflector

Figure 9 The topology optimisation results of the connected plate and cowcatcher deflector

Table 3 provides the max deformation displacement values and compliance responses of the cowcatcher in 4 cases. Analysis reveals a significant reduction in both max deformation displacement values and compliance responses.

Table 3 Optimisation results under multiple working conditions

Case	Pre-optimisation		Post-optimisation	
	Deformation disp. /mm	Compliance response	Deformation disp. /mm	Compliance response
1	7.68	3.335714×10^5	4.67	1.394234×10^5
2	52.32	6.297558×10^6	29.02	3.692036×10^6
3	-6.81	2.283282×10^5	-3.47	1.125999×10^5
4	-9.08	2.687227×10^5	-3.24	1.364337×10^5

4 Sizing optimisation of the cowcatcher

4.1 Sizing optimisation model

To further determine the optimal thickness of the cowcatcher's structural plates based on the preliminary topology optimisation results and to reduce the weight, it is necessary to conduct sizing optimisation for the improved cowcatcher structure.

In the sizing optimisation, the objective function is set to minimize the total mass of the cowcatcher. The design variables include the thicknesses of the cowcatcher deflector, connection rib, central stiffened plate, and hanger base plate, as shown in Figure 10. The values are given in Table 4. Considering that the values in manufacturing generally cannot change continuously, all design variables are defined as discrete variables at once (with an incremental step of 0.1 mm).

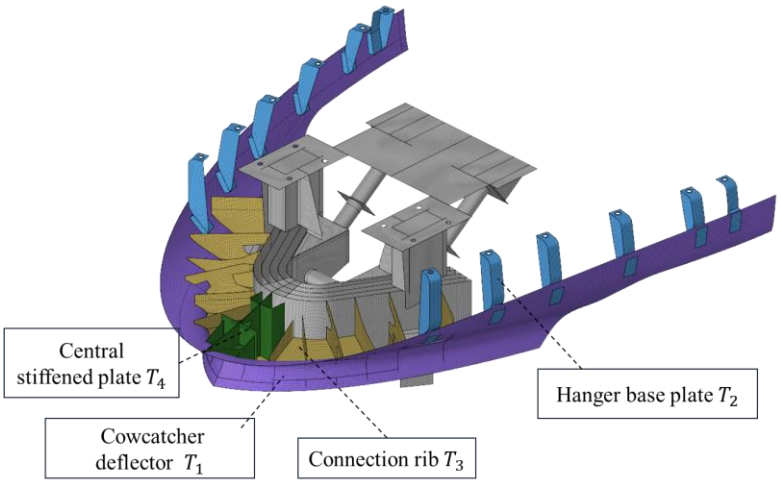

Figure 10 The sizing optimisation model of the cowcatcher

Table 4 The value range of each design variable (unit: mm)

Design variable	Initial thickness	Upper limit	Lower limit
Cowcatcher deflector T_1	6.0	9.0	3.0
Hanger base plate T_2	7.0	10.5	3.5
Connection rib T_3	10.0	15.0	5.0
Central stiffened plate T_4	14.0	21.0	7.0

4.2 Analysis of sizing optimisation results

Figure 11 shows the change curve of the objective function of sizing optimisation with the number of iteration steps, which reaches convergence after 5 iterations. As shown in Table 5, upon convergence of the iterative objective function in step 5, the mass of the cowcatcher has been reduced by 79.65 kg, representing a reduction of 10.43% in mass. The design variables acquired through optimisation have been adjusted in accordance with mechanical design rounding principles to determine the final optimized sizes.

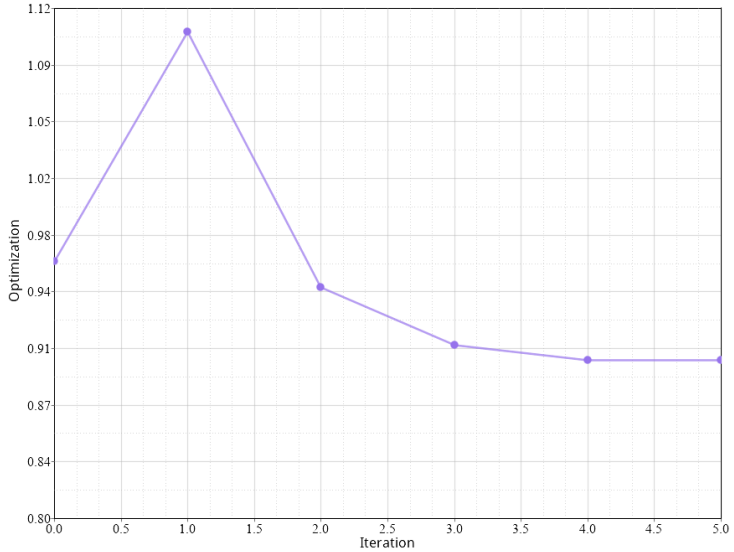

Figure 11 Sizing optimisation objective function iteration curve

Table 5 Design variables and quality changes in each iteration

Iterations	Design variables				Mass change/kg
	T_1/mm	T_2/mm	T_3/mm	T_4/mm	
0	6.0	7.0	10.0	14.0	0
1	6.2	10.5	15.0	21.0	+116.54
2	6.4	10.3	7.5	10.5	-142.86
3	6.2	10.4	6.9	9.1	-38.74
4	6.3	10.5	6.5	9.0	-19.96
5	6.3	10.5	6.5	9.0	0
rounding	6.5	10.5	6.5	9.0	+5.37

5 Comparison and verification

5.1 Simulation conditions settings

Based on the train and track FE models, the cowcatcher models, both pre- and post-optimisation, were assembled onto the car body, and four sets of simulation conditions for train derailment were established for comparative analysis. Two derailment speeds of 36 km/h and 50 km/h were considered, while maintaining a cowcatcher height of 190 mm above the rail top, as shown in Table 6.

Table 6 Parameters of the working conditions

Derail Case	Cowcatcher type	Height /mm	Derailment speed/(km/h)
1	Pre-optimisation	190	36
2	Post-optimisation	190	36
3	Pre-optimisation	190	50
4	Post-optimisation	190	50

5.2 Results and analysis

The results include the post-derailment postures of the vehicle, the kinematic response of the vehicle and the structural response of the cowcatcher. Figure 12 depicts the final postures of the derailed vehicle in 4 cases. As illustrated in Figure 13(a & c), the longitudinal displacements of the carbody with the post-optimized cowcatcher are slightly smaller compared to those with the original structure, measuring 14.22 m in case 1 and 13.86 m in case 2. From Figure 13(b & d), it can be observed that the suppression effect of the optimized cowcatcher on the lateral movement of the train is more pronounced at lower speeds.

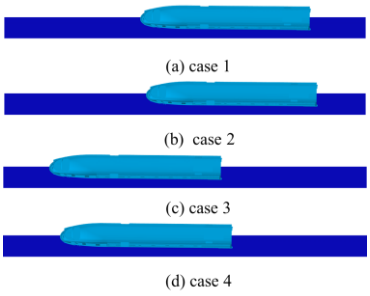

Figure 12 The postures of the derailed vehicle in the 4 cases

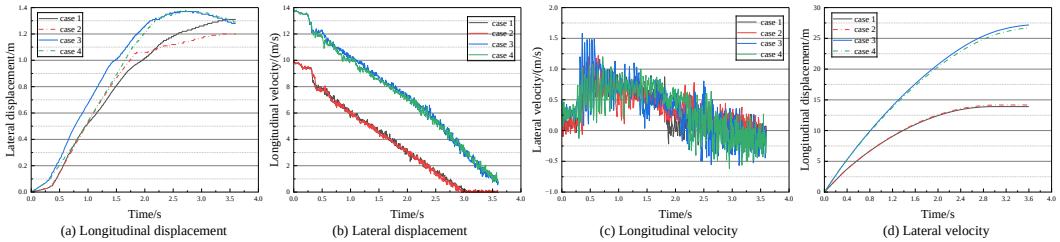

Figure 13 The post-derailment displacements and velocities of the carbody

During the post-derailment, contacts process between the cowcatcher and the rail, primary structural components that undergo deformation are the deflector, connection

plate, and buffer plate. Their respective energy absorptions are depicted in Figure 14(a). Figure 14(b) demonstrates a significant reduction in the maximum stress experienced by the optimized connection plate. In cases 1 and 2, the max stress value decreased from 922 MPa to 783 MPa, marking a reduction of 17.75%. In all cases, the stress exceeds the yield limit, however, since the duration is only 12 ms, the degree of plastic deformation in the structure is relatively limited, as shown in Figure 14(c). In conclusion, the optimisation method notably mitigated stress and strain values on the cowcatcher, thereby fulfilling the initial optimisation design objective.

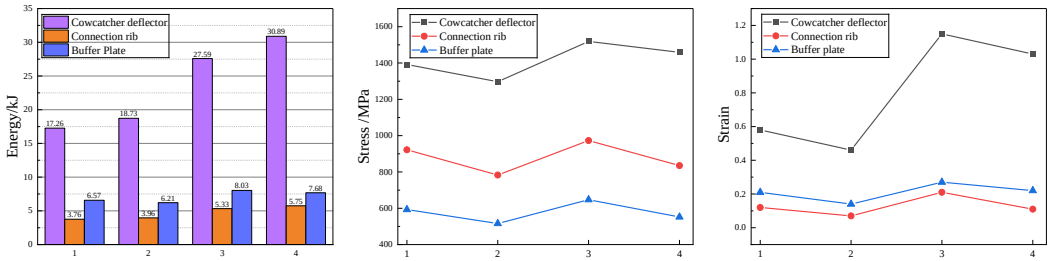

(a) Energy absorption (b) Max von Mises Stress (c) Max equivalent plastic strain

Figure 14 The energy absorptions, stresses and strains of the cowcatcher deflector, connection plate, and buffer plate

6 Conclusions and Contributions

This study conducts a collaborative optimisation involving topology and sizing optimisation for the existing cowcatcher. Subsequent to optimisation, enhancements were made to the cowcatcher's structure, and various post-derailment dynamic collision scenarios were made for comparative analysis, to assess the impact of the optimized cowcatcher on vehicle kinematic response, as well as its structural response.

(1) After topology optimisation, the mass of the cowcatcher decreased by 0.73%. The nodal displacements under various loading conditions decreased by 39.19%, 44.53%, 49.04%, and 64.43%, respectively. The stiffness of the cowcatcher significantly increased after optimisation.

(2) The sizing optimisation design variables include the thickness of the cowcatcher deflector, hanger base plate, connection rib and central stiffened plate. After sizing optimisation, he mass of the cowcatcher decreased by 79.65 kg, with a reduction percentage of 10.43%, yielding a more significant weight reduction compared to topology optimisation.

(3) We constructed multiple post-derailment dynamic collision verification scenarios, and conducted comparative analyses from 3 aspects: the post-derailment postures, kinematic response and cowcatcher structural response. The optimized cowcatcher exhibits enhanced suppression of longitudinal motion, with significant reductions in both maximum stress and strain within its primary load-bearing structures. Consequently, the structural stability of the optimized cowcatcher is notably improved.

Acknowledgements

The authors gratefully acknowledge the support from the National Natural Science Foundation of China (No.52172407, No.U2268210 and No.U19A20110) and the Fundamental Research Funds for the State Key Laboratory of Rail Transit Vehicle System of Southwest Jiaotong University (No.2024RVL-T14).

References

[1] Y. Li, Y. Li, Y. Wang, and J. Wang, "Structural optimization–based fatigue durability analysis of electric multiple units cowcatcher," *Advances in Mechanical Engineering*, vol. 9, no. 8, p. 1687814017726294, Aug. 2017, doi: 10.1177/1687814017726294.

[2] Y. Liu *et al.*, "An investigation into vibration-induced fatigue failure of metro vehicle cowcatcher and its structural improvement design," *Engineering Failure Analysis*, vol. 145, p. 107038, Mar. 2023, doi: 10.1016/j.engfailanal.2022.107038.

[3] S. Y. Li, Z. J. Zheng, and J. L. Yu, "Mechanical Analysis of a Cowcatcher for a High-Speed Train in Crashing," *Applied Mechanics and Materials*, vol. 437, pp. 18–21, 2013, doi: 10.4028/www.scientific.net/AMM.437.18.

[4] Md. I. R. Shishir and A. Tabarraei, "Multi–materials topology optimization using deep neural network for coupled thermo–mechanical problems," *Computers & Structures*, vol. 291, p. 107218, Jan. 2024, doi: 10.1016/j.compstruc.2023.107218.

[5] D. J. Munk, G. A. Vio, and G. P. Steven, "Topology and shape optimization methods using evolutionary algorithms: a review," *Struct Multidisc Optim*, vol. 52, no. 3, pp. 613–631, Sep. 2015, doi: 10.1007/s00158-015-1261-9.

[6] S. D. Rajan, "Sizing, Shape, and Topology Design Optimization of Trusses Using Genetic Algorithm," *Journal of Structural Engineering*, vol. 121, no. 10, pp. 1480–1487, Oct. 1995, doi: 10.1061/(ASCE)0733-9445(1995)121:10(1480).

[7] T. Hirschler, R. Bouclier, A. Duval, T. Elguedj, and J. Morlier, "Isogeometric sizing and shape optimization of thin structures with a solid-shell approach," *Struct Multidisc Optim*, vol. 59, no. 3, pp. 767–785, Mar. 2019, doi: 10.1007/s00158-018-2100-6.

[8] Y. Wan, B. Hu, Y. Yang, F. Jin, J. Zhou, and B. Gao, "Discrete sizing optimization method based on dividing rectangles algorithm and local response surface for steel frame structures," *Journal of Building Engineering*, vol. 79, p. 107826, Nov. 2023, doi: 10.1016/j.jobe.2023.107826.

[9] T. Khatib, A. Mohamed, and K. Sopian, "A review of photovoltaic systems size optimization techniques," *Renewable and Sustainable Energy Reviews*, vol. 22, pp. 454–465, Jun. 2013, doi: 10.1016/j.rser.2013.02.023.

[10] Chen J., Liang X., Xu P., and Che Q., "Windowed design and structure optimization of energy absorbing structure of high-speed train," *Journal of Railway Science and Engineering*, vol. 19, no. 6, pp. 1502–1510, 2022, doi: 10.19713/j.cnki.43-1423/u.t20210632.

[11] T. Kuczek and B. Szachniewicz, “Topology Optimisation of Railcar Composite Structure,” *International Journal of Heavy Vehicle Systems*, vol. 22, no. 4, 2015, Accessed: May 02, 2024. [Online]. Available: https://trid.trb.org/View/1376137
[12] M. Mrzygłód and T. Kuczek, “Uniform crashworthiness optimization of car body for high-speed trains,” *Struct Multidisc Optim*, vol. 49, no. 2, pp. 327–336, Feb. 2014, doi: 10.1007/s00158-013-0972-z.
[13] J. Wang, Y. Zhang, J. Zhang, X. Liang, S. Krajnović, and G. Gao, “A numerical investigation on the improvement of anti-snow performance of the bogies of a high-speed train,” *Proceedings of the Institution of Mechanical Engineers, Part F: Journal of Rail and Rapid Transit*, vol. 234, no. 10, pp. 1319–1334, Nov. 2020, doi: 10.1177/0954409719893494.
[14] Y. Guo, L. Zhang, W. Dou, Y. Zhu, and H. Zhang, “Static strength and crashworthiness analysis of a train cowcatcher at a running speed of 160 km/h,” *High-speed Railway*, vol. 1, no. 4, pp. 258–264, Dec. 2023, doi: 10.1016/j.hspr.2023.11.004.
[15] “An improved integrated framework based nodal density variable and Voronoi polygon for FE-based topology optimization - ScienceDirect.” Accessed: May 02, 2024. [Online]. Available: https://www.sciencedirect.com/science/article/pii/S0045794923002742
[16] A. Tovar, N. M. Patel, G. L. Niebur, M. Sen, and J. E. Renaud, “Topology Optimization Using a Hybrid Cellular Automaton Method With Local Control Rules,” *Journal of Mechanical Design*, vol. 128, no. 6, pp. 1205–1216, Jan. 2006, doi: 10.1115/1.2336251.
[17] G.-J. Park, “Technical overview of the equivalent static loads method for non-linear static response structural optimization,” *Structural and Multidisciplinary Optimization*, vol. 43, no. 3, pp. 319–337, Mar. 2011, doi: 10.1007/s00158-010-0530-x.
[18] M. Bujny, M. Olhofer, N. Aulig, and F. Duddeck, “Topology Optimization of 3D-printed joints under crash loads using Evolutionary Algorithms,” *Struct Multidisc Optim*, vol. 64, no. 6, pp. 4181–4206, Dec. 2021, doi: 10.1007/s00158-021-03053-4.
[19] L. Siva Rama Krishna, N. Mahesh, and N.Sateesh, “Topology optimization using solid isotropic material with penalization technique for additive manufacturing,” *Materials Today: Proceedings*, vol. 4, no. 2, Part A, pp. 1414–1422, Jan. 2017, doi: 10.1016/j.matpr.2017.01.163.
[20] T. Yarlagadda, Z. Zhang, L. Jiang, P. Bhargava, and A. Usmani, “Solid isotropic material with thickness penalization – A 2.5D method for structural topology optimization,” *Computers & Structures*, vol. 270, p. 106857, Oct. 2022, doi: 10.1016/j.compstruc.2022.106857.
[21] N. Gerzen, P. M. Clausen, and C. B. W. Pedersen, “Sizing optimization for industrial applications and best practice design process,” presented at the HPSM/OPTI 2016, Siena, Italy, Sep. 2016, pp. 41–49. doi: 10.2495/HPSM160041.